九州大学学術情報リポジトリ
Kyushu University Institutional Repository

Effects of gas bubbling for shape, size, and composition changes in Au-Ag bimetallic nanoparticles including polygonal Au seeds under oil-bath heating at 150 ℃

Alam, Md. Jahangir
Department of Applied Science for Electronics and Materials, Graduate School of Engineering Sciences, Kyushu University

Tsuji, Masaharu
Institute for Materials Chemistry and Engineering, Kyushu University | Department of Applied Science for Electronics and Materials, Graduate School of Engineering Sciences, Kyushu University

https://hdl.handle.net/2324/25677

出版情報：CrystEngComm. 13 (21), pp.6499-6506, 2011-08-30. RSC Publishing
バージョン：
権利関係：(C) The Royal Society of Chemistry 2011

KYUSHU UNIVERSITY

Effects of gas bubbling for shape, size, and composition changes in Au–Ag bimetallic nanoparticles including polygonal Au seeds under oil-bath heating at 150°C†

Md. Jahangir Alam[a] and Masaharu Tsuji*[a,b]

Effects of Ar or O_2 gas bubbling for shape, size, and composition changes in Au–Ag bimetallic nanoparticles were studied under oil-bath heating at 150°C for 10–60 min in ethylene glycol (EG). When a mixture of polygonal Au seeds, $AgNO_3$, and polyvinylpyrrolidone (PVP) in EG solution was heated from room temperature to 150°C and it was kept at that temperature for 10–60 min under Ar or O_2 gas bubbling, different shape, size, and composition changes were observed. Under Ar gas bubbling, major products after heating for 10 min were polygonal Au core Ag-rich Ag/Au alloy shell particles, denoted as Au@Ag/Au, and spherical Ag-rich Ag/Au alloy particles. They were transformed to larger excentered Au@Ag/Au particles with average diameter of 340±106 nm after further heating for 20–50 min. Under O_2 gas bubbling, major products after heating for 10 min were Au@Ag core–shell particles having a thin Ag shell, large Au-rich Au/Ag alloy particles, and many small spherical Ag particles with 4±2 nm average diameter. After further heating for 20–50 min, the Au@Ag particles fuse and aggregate to form spherical Au-rich Au/Ag alloy particles with average diameter of 259±37 nm. Results show that Ag-rich or Au-rich Au–Ag bimetallic particles can be prepared easily under bubbling Ar or O_2 gas, respectively. The different structure and composition changes in Au–Ag bimetallic particles under Ar or O_2 bubbling are discussed in terms of fusion, aggregation, and oxidative etching of Au and Ag particles.

Introduction

Among many metallic nanostructures, the synthesis of gold nanostructures has been and continues to be an area of active research over the past two decades because of their unique catalytic, optical, electronic, and molecular-recognition properties, which are sought for applications in areas such as catalysis, diagnosis, plasmonics, and surface-enhanced Raman spectroscopy.[1–8] Because properties and applications of colloidal gold nanoparticles depend strongly upon their shape and size, the shape and size-controlled syntheses of gold nanostructures are worthy of investigation.

The shape transformation of gold nanoparticles in solution has been regarded as difficult at low temperatures such as 150°C because gold is inactive and is not dissolved without the presence of a strong acid such as aqua regia. Nevertheless, we found recently that mixtures of octahedral, triangular- and hexagonal-platelike, and decahedral Au nanocrystals with average diameter of 60±10 nm can be converted to monodispersed spherical particles with average diameter of ≈240 nm under bubbling N_2 at 150°C for 10–60 min in ethylene glycol (EG).[9] The rate of shape conversion depends on the gas dissolved in the solvent. It was strongly enhanced in the presence of O_2 in EG.

We discussed the shape changes of Au nanostructures during heating in terms of gas-bubbling-induced Ostwald ripening, shape-selective oxidative etching by O_2/Cl^-, and grain-rotation-induced grain coalescence (GRIGC) and fusion mechanisms.[10] However, definitive evidence is necessary to determine their relative contribution in the shape changes of polygonal gold nanoparticles in EG at low temperatures such as 150°C.

To clarify the origin of shape changes in polygonal Au nanoparticles during oil-bath heating at 150°C, we recently studied the structure and component changes of polygonal Au particles in the presence of Ag components.[11] An advantage of this method is that more direct information related to shape, size, and component changes in Au polygonal particle is obtainable by observing the formation of various kinds of core–shell and Au/Ag alloy nanoparticles during heating. A mixture of polygonal Au seeds, $AgNO_3$, and polyvinylpyrrolidone (PVP) in EG solution, denoted as Au seeds/$AgNO_3$/PVP/EG, was heated from room temperature to 150°C. The mixture was kept at that temperature for 10–60 min. Then, remarkable shape, size, and composition changes were observed for original Au seeds and Au–Ag bimetallic products. After heating for 30 min, Au and Au@Ag core–shell particles attached to Ag-rich Ag/Au alloy nanowires were produced. They were transformed to excentered Au core Ag-rich Ag/Au alloy shell nanoparticles, denoted as Au@Ag/Au, with average diameter of 370±73 nm after further heating for 30 min. Results show that a shape change from Ag/Au alloy nanowires to spherical Ag/Au alloy shells in excentered Au@Ag/Au particles occurs from attached parts of Au and Au@Ag particles to nanowires. That change is explained by the facts that Au and Au@Ag particles attached to nanowires act as defects and that a small amount of Au^{3+} is

released and Ag^0 is dissolved by the reaction.

$$Au^{3+} + 2Ag^0(s) \longrightarrow 2Ag^+ + Au^+ \qquad (1)$$

Because we conducted the experiments described above without gas bubbling, no information related to effects of gas dissolved in EG was obtained for the structure and composition changes in original Au seeds and Au–Ag bimetallic products during heating.

Although gaseous species dissolved in solvent may influence both the reduction kinetics of a precursor and the growth rates of different crystallographic planes under solution phase syntheses of metallic nanoparticles, their presence and potential roles have been largely ignored in most previous studies. Through this study, we examine effects of gas dissolved in EG for shape, size, and composition changes in polygonal Au seeds and Au–Ag bimetallic products during heating of an Au seeds/$AgNO_3$/PVP/EG solution at 150°C under Ar or O_2 gas bubbling. The results were compared with those obtained without gas bubbling.[11] To the best of our knowledge, this is the first study on the effects of gas dissolved in EG for the preparation of Au–Ag bimetallic products in the presence of polygonal Au seeds. We demonstrate here that different shape and composition of Au–Ag bimetallic products can be prepared by changing bubbling gas. The mechanisms of structure and component changes under Ar or O_2 gas bubbling are discussed in terms of fusion, aggregation, and oxidative etching of Au and Ag nanoparticles.

Experimental

Materials and experimental procedures

For use in this study, $HAuCl_4 \cdot 4H_2O$ (>99.0%), $AgNO_3$ (>99.8%) and EG (>99.5%) were purchased from Kishida Chemical Ltd. The PVP powder (average molecular weight M_W: 40k in terms of monomer units) was purchased from Wako Pure Chemical Industries Ltd. Ar (>99.9995%) and O_2 (>99.9%) gases were obtained from Taiyo Nippon Sanso Corp.

Preparation of polygonal Au seeds.

Polygonal Au particles were prepared using the following method. First, 15 mL of EG solution was preheated to 150°C and maintained at this temperature for 60 min by bubbling Ar gas to remove residual water and O_2 dissolved in the solvent. Then a mixture of $HAuCl_4 \cdot 4H_2O$ and PVP (M*w* = 40 k) as a polymer surfactant in 5 mL of EG was added. It was heated further for 10 min at 150°C under bubbling Ar gas. The respective concentrations of $HAuCl_4 \cdot 4H_2O$ and PVP in 20 mL EG solution were 2.4 and 250 mM. The flow rate of Ar was kept at 150 cm^3 min^{-1} using a mass flow controller. The products were collected by centrifugal separation at 12 000 rpm three times for 30 min to remove PVP and all by-products in the supernatant.

Structure and component changes in Au–Ag bimetallic products during heating at 150°C under Ar or O_2 gas bubbling.

An $AgNO_3$ solution containing polygonal Au particles and PVP (M_W: 40k) was prepared in 20 ml EG solution. The concentrations of Au, Ag, and PVP in EG were, respectively, 2.4, 24, and 250 mM. The solution temperature was increased from room temperature to 150°C by heating for 6 min; it was kept at that temperature for 60 min with sampling at 10, 30, and 60 min. Ar or O_2 gas was bubbled into EG solution during heating. The flow rate of Ar or O_2 gas was kept at 150 cm^3 min^{-1} using mass flowmeters.

Analyses of structure, components, and optical properties of products.

For TEM (200 kV, JEM-2000XS; JEOL) observations, Au, Ag, and Au–Ag bimetallic particles were obtained from C_2H_5OH solution by centrifuging the colloidal solution three times at 15 000 rpm for 30 min. The TEM–EDS data (200 kV, 2100F; JEOL) and XRD data (SmartLab; Rigaku) were also measured. Extinction spectra of the product solutions were measured in the UV–vis region using a spectrometer (UV-3600; Shimadzu Corp.).

Results and discussion

Structure and component changes of Au–Ag bimetallic products under Ar gas bubbling

Fig. 1a and Fig. S1 (ESI†) portray typical TEM images of polygonal Au seeds, which consist of a mixture of octahedral, triangular- or hexagonal-platelike, decahedral, and icosahedral particles. The average edge size of octahedral, triangular plate, decahedral, and icosahedral particles was 37±8 nm, essentially independent of the polygonal Au nanocrystal shape. We confirmed in our previous study of crystal structures of these polygonal particles using selected area electron diffraction patterns, and from TEM and SEM images that octahedral particles are single-crystalline, that triangular- and hexagonal-platelike particles are single-twin particles, and that decahedral particles are multiple-twin particles, as shown in Fig. S1 (ESI†).[8] All of these particles have {111} facets as major planes except for hexagonal-platelike particles, where a twin pair of 12 alternative {100} and {111} side facets appear (Fig. S1: ESI†).

Figs. 1b–1d depict typical TEM images of Au–Ag bimetallic product obtained after heating at 150°C for 10, 30, and 60 min, respectively. To confirm Au and Ag distributions in the product particles, TEM–EDS data were measured for products obtained at each heating time (Figs. 2a–2e). Significant shape, size, and composition changes are observed for original Au seeds and Au–Ag bimetallic nanoparticles with increasing heating time. Dominant products at 10 min consist of two components. One is cubic, triangular bipyramidal, and rod types of core–shell particles, having polygonal Au nanoparticles as central cores.[12] TEM–EDS data given in Figs. 2b1–2e1 and Fig. S2 (ESI†) clarify that polygonal Au cores are not covered by pure Ag shells, but they are covered by uniform Ag-rich Ag/Au alloys shells. The atomic ratio of Ag : Au in Ag-rich Ag/Au alloy shell was 99.1±0.3 : 0.9±0.3%. In this stage, the shape and

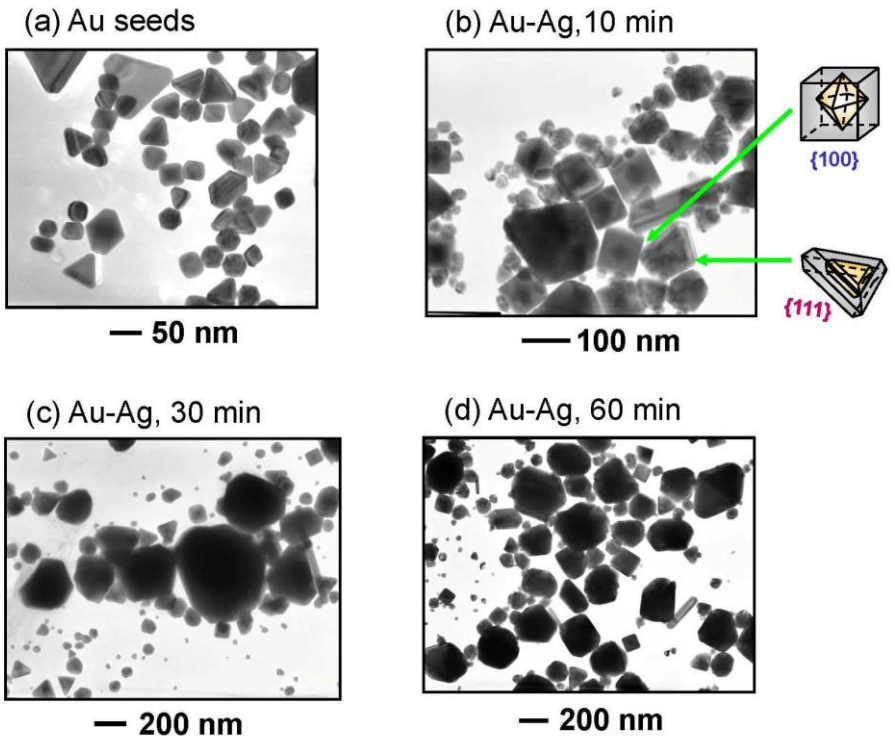

Fig. 1. Typical TEM images of (a) polygonal Au seeds and (b)–(d) Au–Ag bimetallic products after heating Au seeds/$AgNO_3$/PVP/EG solution for 10–60 min under Ar gas bubbling.

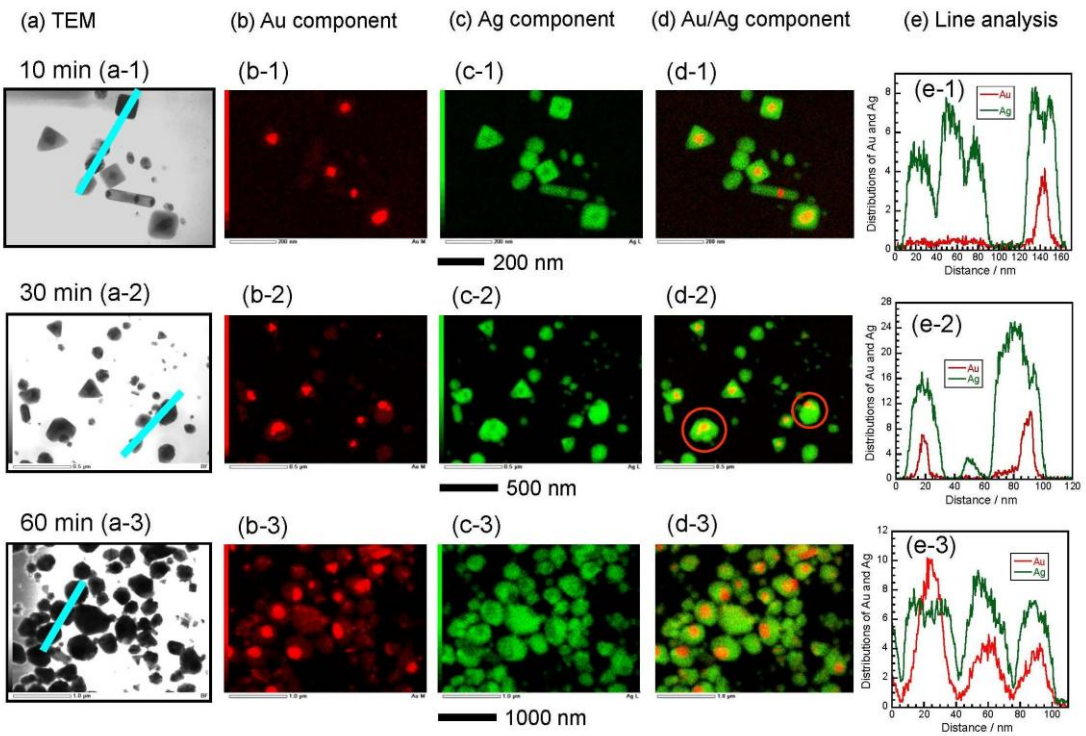

Fig. 2. Typical TEM and TEM–EDS images of Au–Ag bimetallic products obtained after heating Au seeds/$AgNO_3$/PVP/EG solution for 10–60 min under Ar gas bubbling. Figs. 2e1–2e3 are line analysis data along blue lines shown in Figs. 2a1–2a3.

size of initial Au seeds are reserved well as Au cores. The other major product is quasi-spherical particles with average diameter of 27±5 nm. The TEM–EDS data (Figs. 2b1–2e1) show that these spherical particles are Ag-rich Ag/Au alloy particles. The Ag : Au atomic ratio in these Ag/Au alloy particles was 99.2±0.3 : 0.8±0.1%, which was nearly the same as that of Ag/Au shells in Au@Ag/Au particles.

After heating for 30 min, polygonal Au@Ag/Au particles and quasi-spherical Ag/Au alloy particles, as observed at 10 min, are also obtained. In addition, larger quasi-spherical particles with average diameter of 240±47 nm are obtained, as indicated by the red circles in Fig. 2d2. TEM–EDS data (Figs. 2b2–e2) show that quasi-spherical particles are Au core Ag-rich Ag/Au shell nanoparticles, denoted as Au@Ag/Au. The Ag : Au atomic ratio in Ag/Au alloy shells was 99.1±0.4 : 0.9±0.4%. These values were the same as those of Ag/Au shells in Au@Ag/Au core–shell and Ag/Au alloy particles obtained after heating for 10 min. In these Au@Ag/Au particles, Au cores with average size of 132±42 nm do not exist in the center, so spherical particles are not ideal core–shell particles but rather excentered Au@Ag/Au particles.

After heating for 60 min, the number density of excentered Au@Ag/Au particles increases greatly, whereas those of Au@Ag/Au core–shell and Ag/Au alloy particles decrease. The Au : Ag atomic ratio in all products obtained at 60 min heating was 9 : 91, which showed reasonable agreement with that of the initial ratio of 1 : 10. The average size of excentered Au@Ag/Au particles increases from 240±47 nm to 340±106 nm with increasing heating time from 30 to 60 min. We obtained similar Au@Ag/Au particles using a similar experiment without gas bubbling.[11] The average sizes of Au@Ag/Au particles obtained at 60 min heating in this study under Ar gas bubbling were similar to that obtained without gas bubbling: 370±73 nm.[11]

In order to obtain information on c rystal structures of excentered Au@Ag/Au particles, their XRD patterns were measured (Fig. S3a: ESI†). Owing to the same fcc crystal structure and similar lattice constants between Au core and Ag/Au alloy shell particles show the similar diffraction peaks which are overlapped with each other. Prominent diffraction peaks were indexed to the {111}, {200}, {220}, {311}, and {222} planes of Au and Ag/Au particles with fcc structure: e.g. PDF 01-071-9134. The peak intensity of {111} facet is strongest, indicating that the favorable facet of Au@Ag/Au particles is {111}. Sharp peaks observed in Au@Au/Ag particles without amorphous components suggest that these particles are polycrystals.

UV–Vis spectra under Ar gas bubbling

UV–vis spectra were measured to characterize optical properties and to examine the time evolution of Au–Ag bimetallic particles. Fig. 3 portrays UV–vis spectra obtained before heating and after heating at 150°C for 2–60 min under Ar gas bubbling. A broad surface plasmon resonance (SPR) band of Au polygonal seeds is observed in the 500–800 nm region with a peak at ≈640 nm before heating of the Au seeds/$AgNO_3$/PVP/EG solution. After heating for 2 min, although the broad SPR band of Au polygonal band decreases greatly, a symmetrical SPR band of Ag component appears in the 320–500 nm with a peak at ≈410 nm. When Ag nanoparticles were prepared from an $AgNO_3$/PVP/EG solution without addition of Au seeds in oil-bath heating at 150°C, spherical Ag particles with average diameter of ≈19±2 nm were obtained (Fig. S4a: ESI†). They gave a typical SPR band of spherical Ag nanoparticles in the 320–500 nm region with a peak at ≈410 nm (Fig. S4b: ESI†). The observed wavelength of the UV–vis spectrum after heating for 2 min was similar to that observed in pure Ag nanoparticles. It is noteworthy that the intensity of the SPR band of Au component decreased greatly, indicating that polygonal Au particles are nearly fully covered by the Ag component after heating for only 2 min. With increasing heating time from 2 min to 10–30 min, the intensity of SPR increased. The SPR band became broad because of the appearance of a long tail band of Au component above 500 nm. The peak shifted to red from 410 nm to 440 nm. The peaks of the SPR band of Au@Ag/Au core–shell particles and Ag/Au alloy particles are known to shift to red and become broad relative to that of pure Ag nanoparticles.[5,13–16] The red shift and broadening of the SPR band in this study are consistent with the fact that the dominant products are Au@Ag/Au core–shell and Ag/Au alloy particles after heating for 10 min and few pure Ag nanoparticles are formed. After heating for 30–60 min, only slight changes in the spectral features were observed, indicating that only slight changes in optical properties of the Au–Ag bimetallic products occur in this time range.

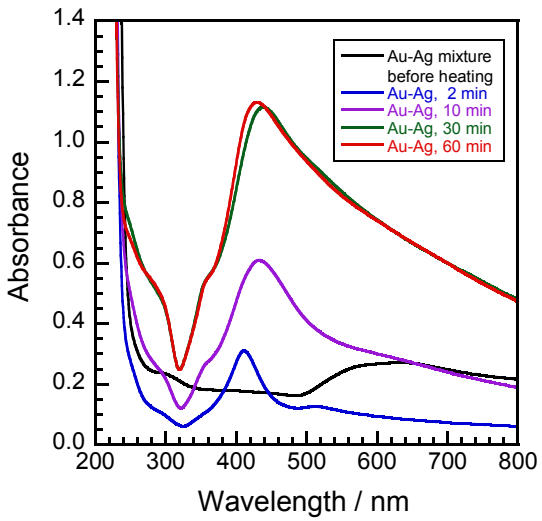

Fig. 3. Spectral changes of Au–Ag bimetallic products obtained before and after heating Au seeds/$AgNO_3$/PVP/EG solution under Ar gas bubbling.

Structure and component changes in Au–Ag bimetallic products under O_2 bubbling

Figs. 4a–4d portray typical TEM images of Au seeds and Au–Ag bimetallic products obtained after heating Au seeds/$AgNO_3$/PVP/EG solution under O_2 bubbling at 150°C for 10, 30, and 60 m in, respectively. Figs. 5a1–5e3 show TEM, TEM–EDS, and their line analysis data at each

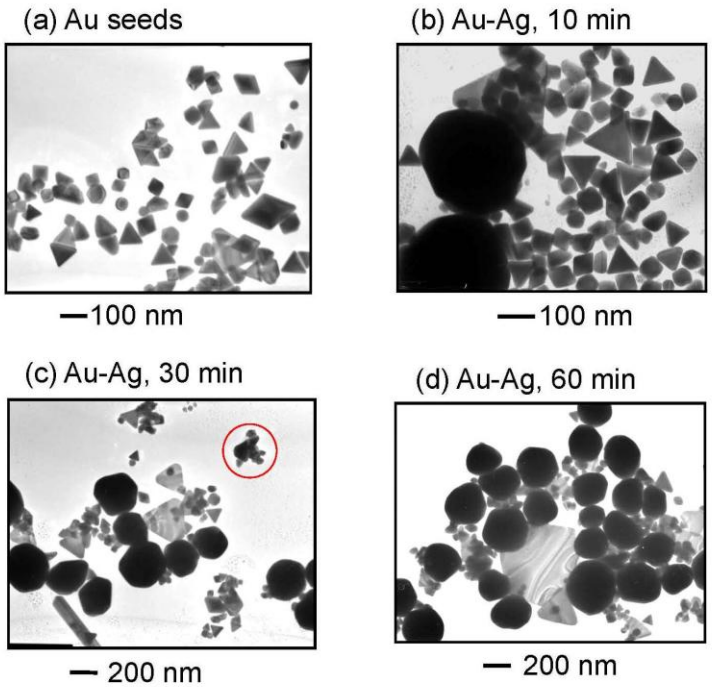

Fig. 4. Typical TEM images of (a) polygonal Au seeds and (b)–(d) Au–Ag bimetallic products obtained after heating Au seeds/$AgNO_3$/PVP/EG solution for 10–60 min under O_2 gas bubbling.

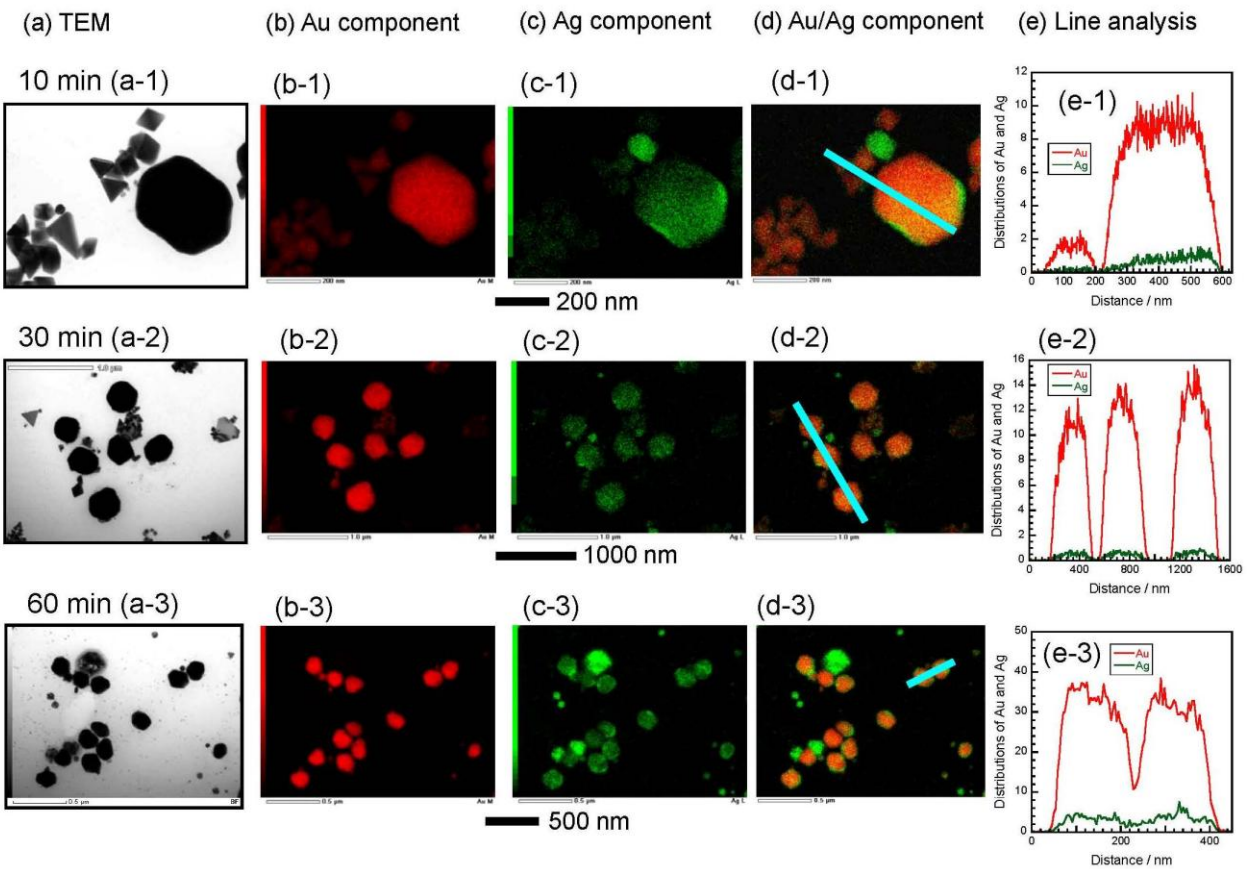

Fig. 5. Typical TEM and TEM–EDS images of Au–Ag bimetallic products obtained after heating Au seeds/$AgNO_3$/PVP/EG solution under O_2 gas bubbling. Figs. 5e1–5e3 are line analysis data along blue lines shown in Figs. 5d1–5d3.

heating time. Major products after 10 min heating are polygonal particles, which have similar shapes and sizes to those of Au seeds. In addition, small quantities of large spherical particles are obtained (Figs. 4b and 5a1–5d1). Based on TEM–EDS data presented in Figs. 5a1–5e1, polygonal particles are Au@Ag core–shell particles, which consist of polygonal Au core seeds and thin Ag shells having the same shapes as those of Au cores. On the other hand, large spherical particles are Au-rich Au/Ag alloy particles. The Au : Ag atomic ratios of Au@Ag core–shell and Au/Ag alloy particles were 90 : 10 and 87 : 13, respectively.

After heating for 30–60 min, polygonal Au@Ag core–shell particles are converted to large spherical Au-rich Au/Ag alloy particles by fusion and aggregation processes, as shown by a red circle in Fig. 4c. Therefore, the number density of large spherical Au/Ag alloy particles increases concomitantly with increasing heating time from 30 min to 60 min. The average size of spherical Au/Ag alloy particles was 259±37 nm and the atomic ratio of Au : Ag was 88 : 12. This Au : Ag atomic ratio is markedly different from that of the initial Au : Ag ratio of 1 : 10 in reagents, where a large excess amount of Ag reagent was added.

To clarify a reason for this large discrepancy in Au : Ag atomic ratio between reagents and products, we re-examined TEM images in greater detail. Figs. S5–S7 (ESI†) depict typical expanded TEM. The TEM–EDS data are measured at higher contrast to show small light contrast particles at heating times of 2, 10, and 30 min. It is noteworthy that small particles with average size of 4±2 nm are formed even at a short heating time of 2 min and that they remain after heating for 30 and 60 min. Apparently, collection of all these small particles through centrifugal separation is difficult. Consequently, the high Au/Ag ratio observed in Au–Ag bimetallic products under O_2 gas bubbling can be attributed to the formation of many small Ag particles. When TEM images of Au–Ag bimetallic products under Ar gas bubbling were measured at higher contrast than those presented in Figs. 1 and 2, such small Ag particles were not observed. Therefore, the formation of many small Ag nanoparticles is an outstanding feature of products under O_2 gas bubbling. To examine further whether small Ag nanoparticles are formed only in the presence of Au seeds or produced without the presence of Au seeds, Ag nanoparticles were prepared from an $AgNO_3$/PVP/EG solution under O_2 gas bubbling without addition of polygonal Au seeds. Results demonstrated that, aside from spherical Ag nanoparticles with average diameter of 42±14 nm, many small spherical Ag particles with average size of 4±1 nm were formed (see red circles in Fig. S8: ESI†). Such small particles were not formed from the same $AgNO_3$/PVP/EG solution under Ar gas bubbling. Consequently, the formation of small Ag nanoparticles is an aspect of the intrinsic nature of Ag nanoparticles prepared from the $AgNO_3$/PVP/EG solution under O_2 gas bubbling, independent of the presence of polygonal Au seeds.

We measured XRD patterns of products obtained after heating for 60 min under O_2 gas bubbling (Fig. S3b: ESI†). Major diffraction peaks of mixtures of spherical Au-rich Au/Ag alloy particles and small Ag particles were the same as those obtained under Ar gas bubbling, although the relative intensity of {111} peak to those of other peaks is stronger than that in the case of Ar gas bubbling. These results indicate that products consist of polycrystals of Au/Ag and Ag nanoparticles with fcc structure.

UV–Vis spectra of products under O_2 gas bubbling

Fig. 6 depicts UV–vis spectra of the Au seeds/$AgNO_3$/PVP/EG solution before heating and Au–Ag bimetallic products obtained after heating at 150°C for 10, 30, and 60 min. A broad SPR band of Au polygonal seeds is observed in the 500–800 nm region with a peak at ≈560 nm before heating. After heating for 10 min, the SPR band shifts to blue by ≈20 nm; only a slight increase in the peak intensity is observed. Only slight changes in the peak position and intensity of the Au component are observed during heating for 10–60 min. However, a strong SPR band of Ag component appears in the 320–480 nm region with a peak at ≈410 nm after heating for 10–60 min, although the intensity change for the heating time was opposite to that under Ar bubbling. The intensity of the Ag component decreased with increasing heating time from 10 min to 30 min. After further heating for 30 min, it decreased further. The Ag component became broad and its peak shifted to ≈420 nm because of the increase in the number density of Au-rich Au/Ag alloy particles.

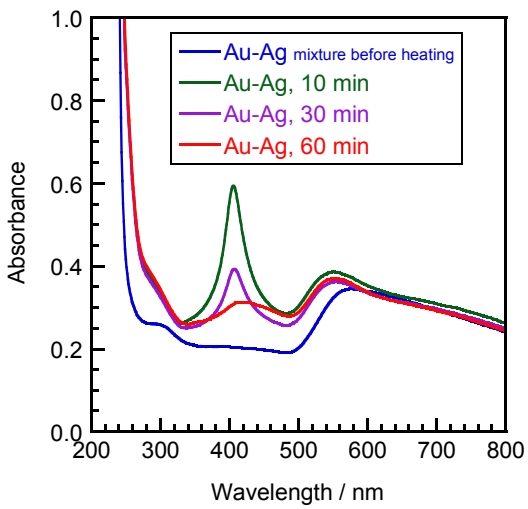

Fig. 6. Spectral changes of Au–Ag bimetallic products obtained before and after heating Au seeds/$AgNO_3$/PVP/EG solution under O_2 gas bubbling.

Mechanisms of structure and composition changes in Au–Ag bimetallic systems under Ar or O_2 gas bubbling

The present results show that shape, size, and composition changes of the Au–Ag bimetallic system during heating for 10–60 min gave different products under bubbling Ar or O_2 gas. Figs. 7 and 8 present schematic processes for shape, size, and composition changes of Au–Ag bimetallic system during heating at 150°C under Ar or O_2 gas bubbling. Under Ar gas bubbling, a mixture of polygonal Au@Ag/Au core–

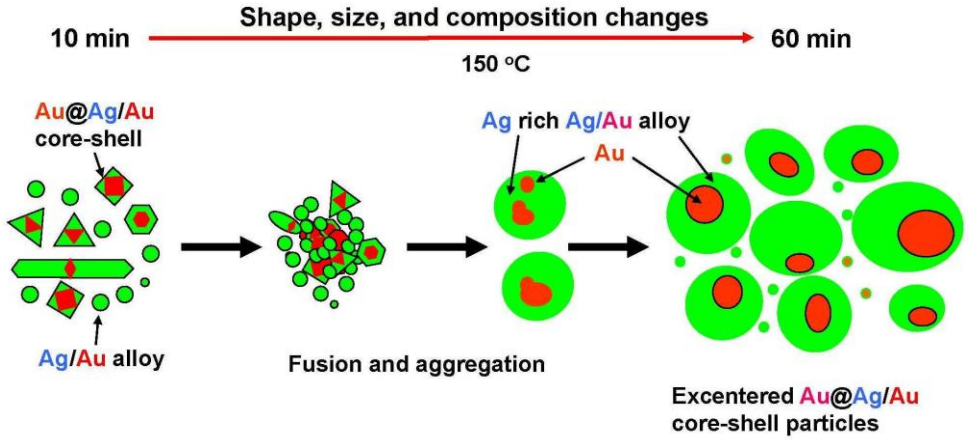

Fig. 7. Schematic process for shape, size, and composition changes in Au–Ag bimetallic products obtained after heating Au seeds/$AgNO_3$/PVP/EG solution under Ar gas bubbling.

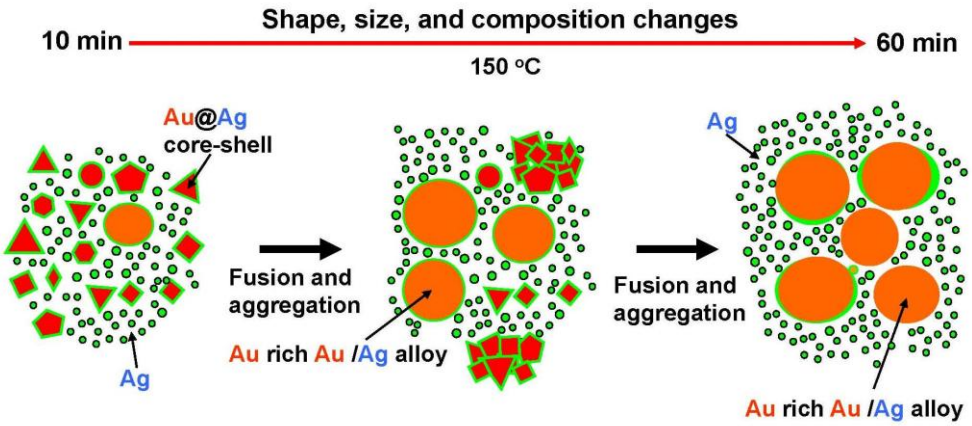

Fig. 8. Schematic process for shape, size, and composition changes in Au–Ag bimetallic products obtained after heating Au seeds/$AgNO_3$/PVP/EG solution under O_2 gas bubbling.

shell particles having well defined {100} facets and spherical Ag/Au alloy particles were formed after 10 min heating. It is noteworthy that small amounts (about 1%) of Au components are distributed uniformly in the shell part of Au@Ag/Au particles and spherical Ag-rich Ag/Au alloy particles, as shown in high contrast TEM–EDS data in Fig. 2b1–2b3 and Fig. S2b (ESI†). These facts imply that Ag^+ ions and also a small amount of Au^{3+} ions were reduced simultaneously, forming uniform Ag-rich Ag/Au alloy shells in Au@Ag/Au particles and Ag-rich Ag/Au alloy particles under Ar gas bubbling during heating from room temperature to 150°C for 6 m in while maintaining this temperature for 10 min. Apparently, a small amount of Au^{3+} is released from the polygonal Au particles because of dissolution of Au particle surfaces in the presence of H^+ and NO_3^- ions without the assistance of O_2. In our conditions, H^+ ions are formed by reduction of Ag^+ in EG.[8]

$$CH_2OH\text{-}CH_2OH \rightarrow CH_3CHO + H_2O \quad (2)$$

$$2CH_3CHO + Ag^+ \rightarrow 2Ag^0 + 2H^+ + CH_3COCOCH_3 \quad (3)$$

Additionally, NO_3^- ions come from electrolytic dissociation of $AgNO_3$. Consequently, a small amount of Au^{3+} ions is released in the initial stage, where Au@Ag/Au particles and Ag/Au alloys are formed. After heating for 30–60 min, Au@Ag/Au core–shell and Ag/Au alloy particles are fused and aggregated to larger excentered Au@Ag/Au particles to reduce the total surface energy (Ostwald ripening). The TEM–EDS data show that multiple Au core and Ag/Au alloy shell particles are formed by fusion and aggregation of Au@Ag/Au core–shell and Ag/Au alloy particles as intermediates of excentered Au@Ag/Au particles at 30 min (see red circles in Fig. S9: ESI†). After further heating for 30 min, multiple Au cores are fused and aggregated to phase-separated excentered Au@Ag/Au core–shell particles. The atomic ratio of Au in Ag-rich Ag/Au alloy shells in Au@Ag/Au core–shell particles obtained at 10 m in heating and Ag-rich Ag/Au shells in Au@Ag/Au particles obtained at 30–60 min heating are nearly equal. These facts led us to conclude that fusion and aggregation of multiple Au cores

leading to a larger spherical Au core occur, although alloying between multiple Au cores and Ag-rich Ag/Au shells leading to Au enriched Ag/Au alloy shells does not take place during 30–60 min heating under Ar gas bubbling. When Au@Ag/Au particles grow to a critical size (≈350 nm), they become stable for thermal annealing so that monodispersed sizes of Au@Ag/Au particles are finally produced under Ar gas bubbling.

Formation of excentered Au core Ag-rich Ag/Au alloy shell nanoparticle under Ar gas bubbling is similar to that without gas bubbling.[11] However, the formation process without gas bubbling is significantly different from that under Ar gas bubbling. For the case without gas bubbling, major precursors of excentered Au@Ag/Au particles are Au and Au@Ag core–shell particles attached to Ag-rich Ag/Au alloy nanowires.[11] On the other hand, major precursors are Au@Ag/Au core–shell and Ag/Au alloy particles under Ar gas bubbling. In both cases, they are transferred to excentered Au@Ag/Au particles with average diameters of 355±15 nm by fusion and aggregation of intermediates. The absence of Ag/Au nanowires under Ar gas bubbling implies that a small amount of O_2 dissolved in EG is necessary for the formation of Ag/Au nanowires in the intermediate stage.

Under O_2 gas bubbling, polygonal Au@Ag core–shell particles having thin Ag shells are produced after heating for 10 min (Fig. 8). In addition, many small Ag nanoparticles are formed. The formation of small Ag nanoparticles under O_2 bubbling is part of the intrinsic nature of Ag nanoparticles under O_2 bubbling. After heating for 30–60 min, Au@Ag particles are fused and mutually aggregated, thereby producing larger spherical Au-rich Au/Ag alloy particles. The TEM–EDS data show that the relative distribution of Ag component to that of Au one in Au/Ag alloy particles increases from the inside to the outside of the particles (Figs. 5e2 and 5e3), which implies that alloying between Au cores and Ag shells does not occur completely during fusion and aggregation under O_2 gas bubbling. An important finding of this study is that O_2 is necessary for alloying between Au cores and Ag or Ag-rich Ag/Au alloy shell by heating at 150°C in EG.

If Ostwald ripening dominates the shape, size, and component changes for small Ag nanoparticles, then they are fused and aggregated to form large Ag particles. However, they are formed at the initial stage at 10 min and remain during heating for 30–60 min. The oxidative etching of Ag particles assisted by O_2 might suppress the formation of large Ag nanoparticles.

Conclusion

Shape changes in polygonal Au nanocrystals in the presence of Ag^+ ions were examined during oil-bath heating at 150°C in EG solution for 10–60 min under Ar or O_2 gas bubbling. Shape, size, and composition changes of Au–Ag bimetallic nanoparticles depend strongly on the bubbling gas. Under Ar gas bubbling, excentered Au core Ag-rich Ag/Au shell particles are formed through fusion and aggregation of polygonal Au core Ag-rich Ag/Au shell particles. Under O_2 gas bubbling, Au-rich Au/Ag alloy particles were formed as major products. In addition, small Ag nanoparticles were formed and remained even after 60 min heating. Because large Au/Ag alloy and small Ag particles can be separated easily through centrifugal separation, the present method constitutes a new promising method for the preparation of monodispersed Au-rich Au/Ag alloy particles under O_2 gas bubbling. The most outstanding result is that the major composition of Au–Ag bimetallic products can be changed from Ag-rich to Au-rich particles by changing the bubbling gas from Ar to O_2 in EG solution.

Acknowledgements

We thank Messrs. Takeshi Tanaka and Taisuke Matsumoto and Mrs. Mika Matsunaga for their help in TEM–EDS and XRD measurements. This work was supported by a Grant-in-Aid for Scientific Research (B) from the Ministry of Education, Culture, Sports, Science, and Technology of Japan (MEXT, No. 22310060), by Management Expenses Grants for National Universities Corporations from MEXT, and the Kyushu Univ. GCOE program "Novel Carbon Resource Sciences." M. J. Alam gratefully acknowledges a Kuma Scholarship and the Graduate School of Engineering Science, Kyushu University for financial support.

Notes and references

[a] Department of Applied Science for Electronics and Materials, Graduate School of Engineering Sciences, Kyushu University, Kasuga 816-8580, Japan

[b] Institute for Materials Chemistry and Engineering, Kyushu University, Kasuga 816-8580, Japan. E-mail:tsuji@cm.kyushu-u.ac.jp; Fax: +81-092-583-7815; Tel.: +81-092-583-7815

† Electronic Supplementary Information (ESI) available: TEM, TEM–EDS, XRD, and UV–vis data obtained using various experimental methods at various reaction stages are presented by the authors. See DOI:

1 M. C. Daniel and D. Astruc, *Chem. Rev*., 2004, **104**, 293.

2 B. Nikoobakht and M. A. El-Sayed, *Chem. Mater*., 2003, **15**, 1957.

3 C. J. Murphy, *Science*, 2002, **298**, 2139; N. R. Jana, L. Gearheart, S. O. Obare and C. J. Murphy, *Langmuir*, 2002, **18**, 922; C. J. Murphy, T. K. Sau, A. M. Gole, C. J. Orendorff, J. Gao, L. Gou, S. E. Hunyadi and T. Li, *J. Phys. Chem.*, *B*, 2005, **109**, 13857; C. J. Murphy, A. M. Gole, E. Simona, A. E. Hunyadi and C. J. Orendorff, *Inorg. Chem.*, 2006, **45**, 7544.

4 J. Rodríguez-Fernández, J. Pérez-Juste, P. Mulvaney and L. M. Liz-Marzán, *J. Phys. Chem., B*, 2005, **109,** 14257; A. Sánchez-Iglesias, I. Pastoriza-Santos, J. Pérez-Juste, B. Rodríguez-González, F. J. García de Abajo and L. M. Liz-Marzán, *Adv. Mater*., 2006, **18**, 2529; M. Grzelczak, J. Pérez-Juste, P. Mulvaney, and L. M. Liz-Marzán, *Chem. Soc. Rev*., 2008, **37**, 1783.

5 M. Hu, J. Chen, Z.-Y. Li, L. Au, G. V. Hartland, X. Li, M. Marquez and Y. Xia, *Chem. Soc. Rev*., 2006, **35**, 1084; Y. Xia, Y. Xiong, B. Lim and S. E. Skrabalak, *Angew. Chem. Int. Ed*., 2009, **48**, 60.

6 X.-L. Tang, P. Jiang, G.-L. Ge, M. Tsuji, S.-S. Xie and Y.-J. Guo, *Langmuir*, 2008, **24**, 1763.

7 J. E. Millstone, S. J. Hurst, G. S. Métraux, J. I. Cutler and C. A. Mirkin, *Small*, 2009, **5**, 646.

8 M. Tsuji, M. Hashimoto, Y. Nishizawa and T. Tsuji, *Chem. Lett*., 2003, **32**, 1114; M. Tsuji, M. Hashimoto, Y. Nishizawa, M. Kubokawa and T. Tsuji, *Chem. Eur. J*., 2005, **11**, 440; M. Tsuji, N. Miyamae, M. Hashimoto, M. Nishio, S. Hikino, N. Ishigami and I. Tanaka, *Coll. & Surf. A*, 2007, **302**, 587; M. Tsuji, N. Miyamae, M. Nishio, S. Hikino and N. Ishigami, *Bull. Chem. Soc. Jpn.*, 2007, **80**, 2024; M. Tsuji, D. Ueyama, M. J. Alam and S. Hikino, *Chem. Lett*.,

2009, **38**, 478; M. Tsuji, D. Ueyama and M. J. Alam, *Chem. Lett*., 2009, **38**, 618.
9 M. J. Alam, M. Tsuji and M. Matsunaga, *Bull. Chem. Soc. Jpn.*, 2010, **83**, 92.
10 E. R. Leite, T. R. Giraldi, F. M. Pontes, E. Longo, A. Beltrán and J. Andrés, *Apply. Phys. Lett*., 2003, **83**, 1566.
11 M. J. Alam, M. Tsuji, M. Matsunaga and D. Yamaguchi, *CrystEngCommm*, 2011, **13**, 2984 (2011).
12 M. Tsuji, N. Miyamae, S. Lim, K. Kimura, X. Zhang, S. Hikino and M. Nishio, *Cryst. Growth Des*., 2006, **6**, 1801; M. Tsuji, M. Nishio, P. Jiang, N. Miyamae, S. Lim, K. Matsumoto, D. Ueyama and X.-L. Tang, *Colloids Surf., A*, 2008, **317**, 247; M. Tsuji, R. Matsuo, P. Jiang, N. Miyamae, D. Ueyama, N. Nishio, S. Hikino, H. Kumagae, K. S. N. Kamarudin and X.-L. Tang, *Cryst. Growth Des*., 2008, **8**, 2528; M. Tsuji, M. Ogino, M. Matsunaga, N. Miyamae, R. Matsuo, M. Nishio and M. J. Alam., *Cryst. Growth Des*., 2010, **10**, 4085; X.-L. Tang and M. Tsuji, *CrystEngComm*, 2011, **11**, 72.
13 X.-L. Tang, M. Tsuji, P. Jiang, M. Nishio, S.-M. Jang and S.-H. Yoon, *Colloids Surf., A*, 2009, **338**, 33; X. -L. Tang, M. Tsuji, M. Nishio and P. Jiang, *Bull. Chem. Soc. Jpn*., 2009, **82**, 1304; X.-L. Tang and M. Tsuji, in *Nanowires*, 2010, Lupu, N. Ed. IN-TECH Web book, Chap. 2, pp. 25-42.
14 J. H. Hodak, A. Henglein, M. Giersig and G. V. Hartland, *J. Phys. Chem., B*, 2000, **104**, 11708; S. P. Chandran, J. Ghatak, P. V. Satyam and M. Sastry, *J. Colloid Int. Sci*., 2007, **312**, 498.
15 M. Hu, J. Chen, Z. -Y. Li, L. Au, G. V. Hartland, X. Li, M. Marquez and Y. Xia, *Chem. Soc. Rev*., 2006, **35**, 1084.
16 B. Wiley, S.-H. Im, Z.-H. Li, J. M. McLellan, A. Siekkinen and Y. Xia, *J. Phys. Chem., B*, 2006, **110**, 15666.

Synopsis for Graphical Abstract

Excentered Au core Ag-rich Ag/Au alloy shell or Au-rich Au/Ag alloy particles were prepared after heating $AgNO_3$/PVP/ethylene glycol solution involving polygonal Au nanocrystals under oil-bath heating under Ar or O_2 gas bubbling.

Figure for Graphical Abstract

Figure for TOC: M. J. Alam

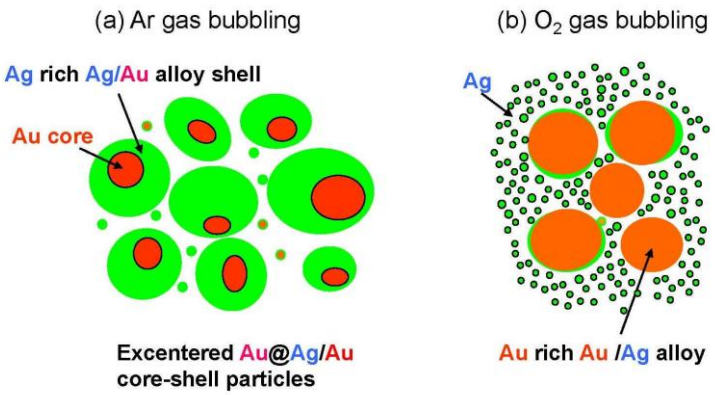

Supplementary Information

Effects of gas bubbling for shape, size, and composition changes in Au–Ag bimetallic nanoparticles including polygonal Au seeds under oil-bath heating at 150° C

Md. Jahangir Alam[a] and Masaharu Tsuji*[a,b]

[a] *Department of Applied Science for Electronics and Materials, Graduate School of Engineering Sciences, Kyushu University, Kasuga 816-8580, Japan*

[b] *Institute for Materials Chemistry and Engineering, Kyushu University, Kasuga 816-8580, Japan*

**To whom correspondence should be addressed: E-mail: tsuji@cm.kyushu-u.ac.jp*

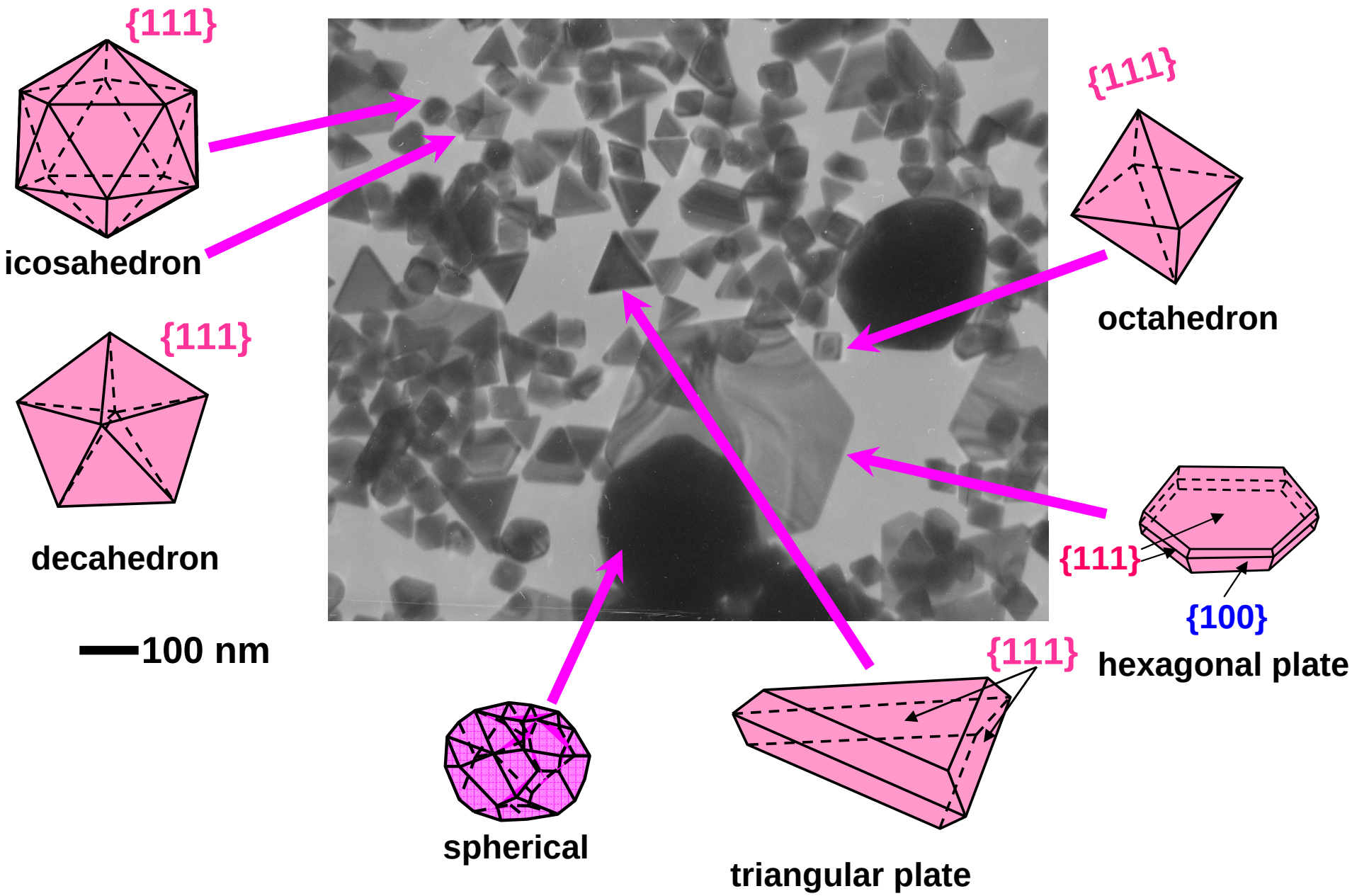

Fig. S1. TEM image of typical polygonal Au seeds and their crystal structures.

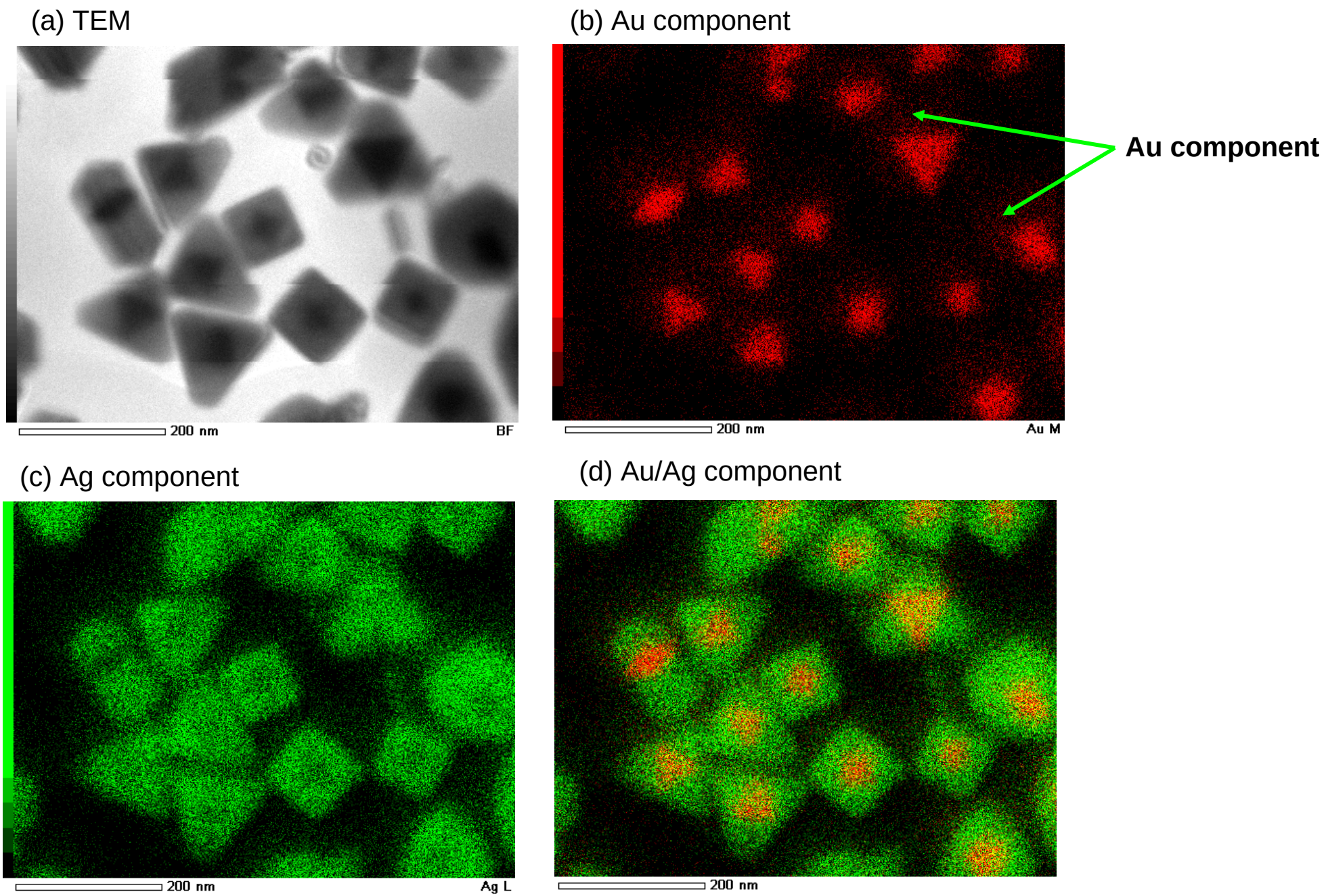

Fig. S2. TEM and TEM–EDS data of Au@Ag/Au nanoparticles obtained from Au seeds/$AgNO_3$/PVP/EG solution after heating for 10 min under Ar gas bubbling.

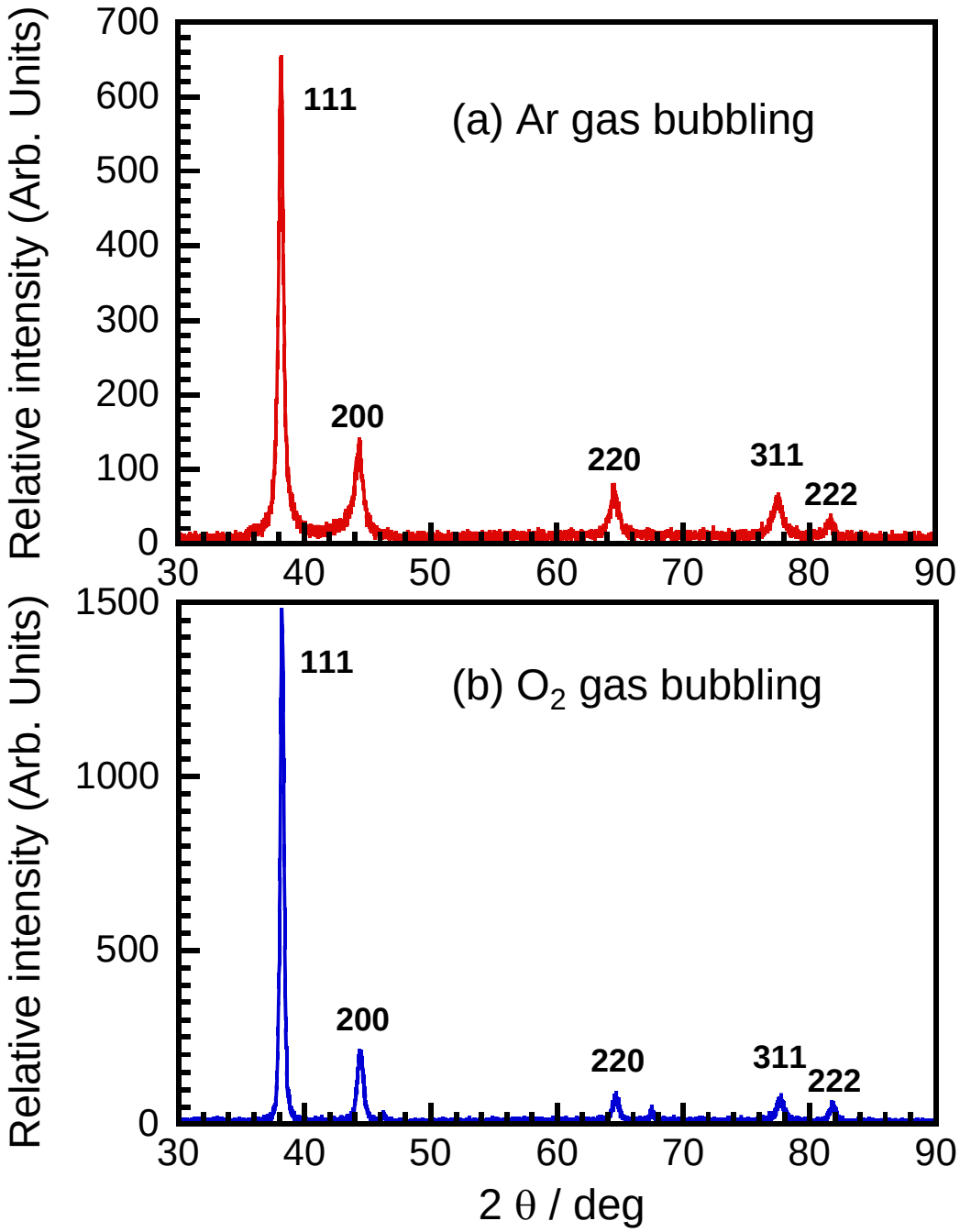

Fig. S3. XRD patterns of Au–Ag bimetallic particles obtained from Au seeds/ $AgNO_3$/ PVP/EG solution after heating for 60 min under (a) Ar gas bubbling and (b) O_2 gas bubbling.

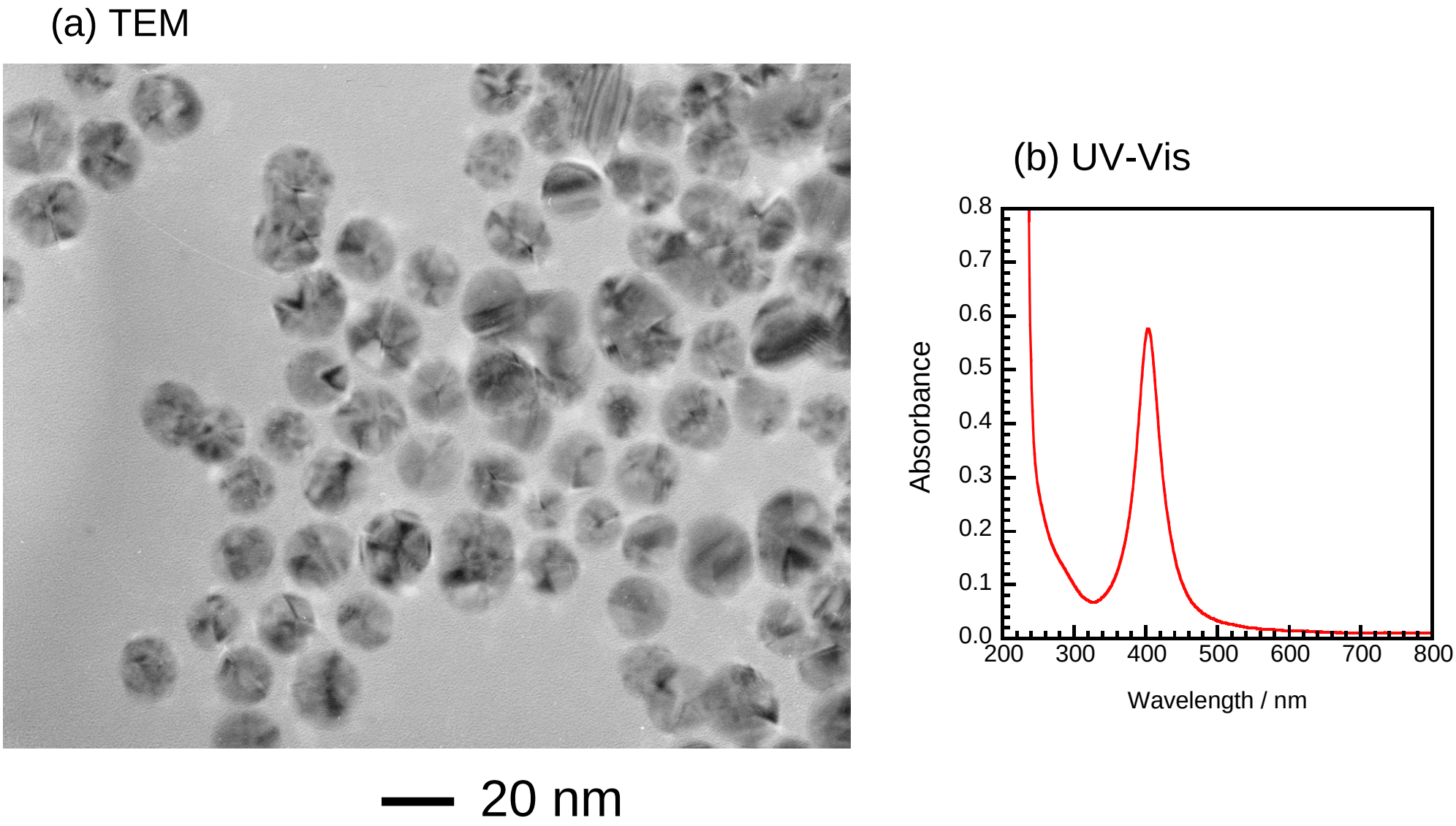

Fig. S4. (a) TEM image and (b) UV-vis spectrum of Ag nanoparticles obtained from $AgNO_3$/PVP/EG solution after heating for 10 min under Ar gas bubbling.

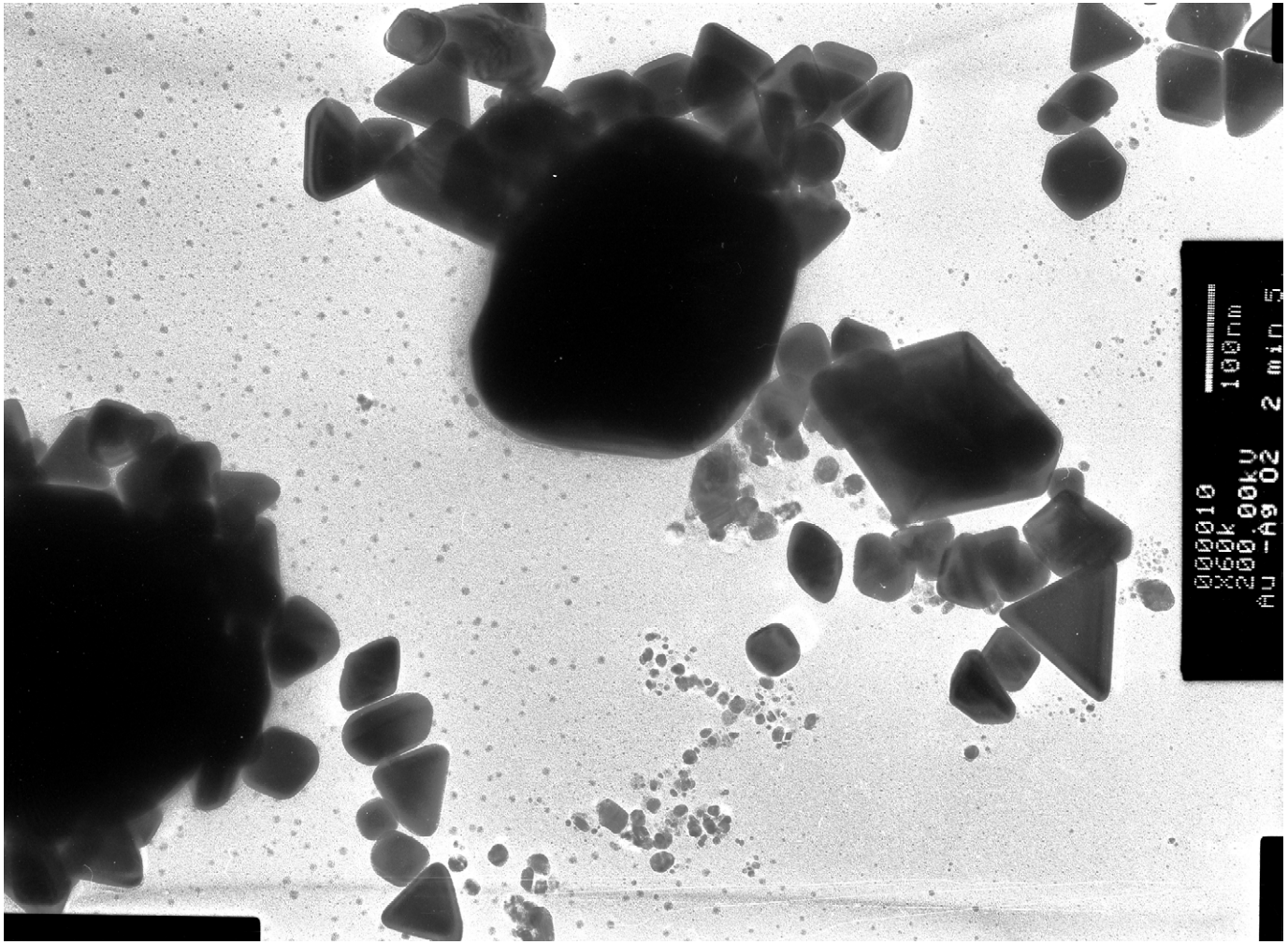

Fig. S5. TEM image of Au–Ag bimetallic products obtained from Au seeds/$AgNO_3$/ PVP/EG solution after heating for 2 min under O_2 gas bubbling.

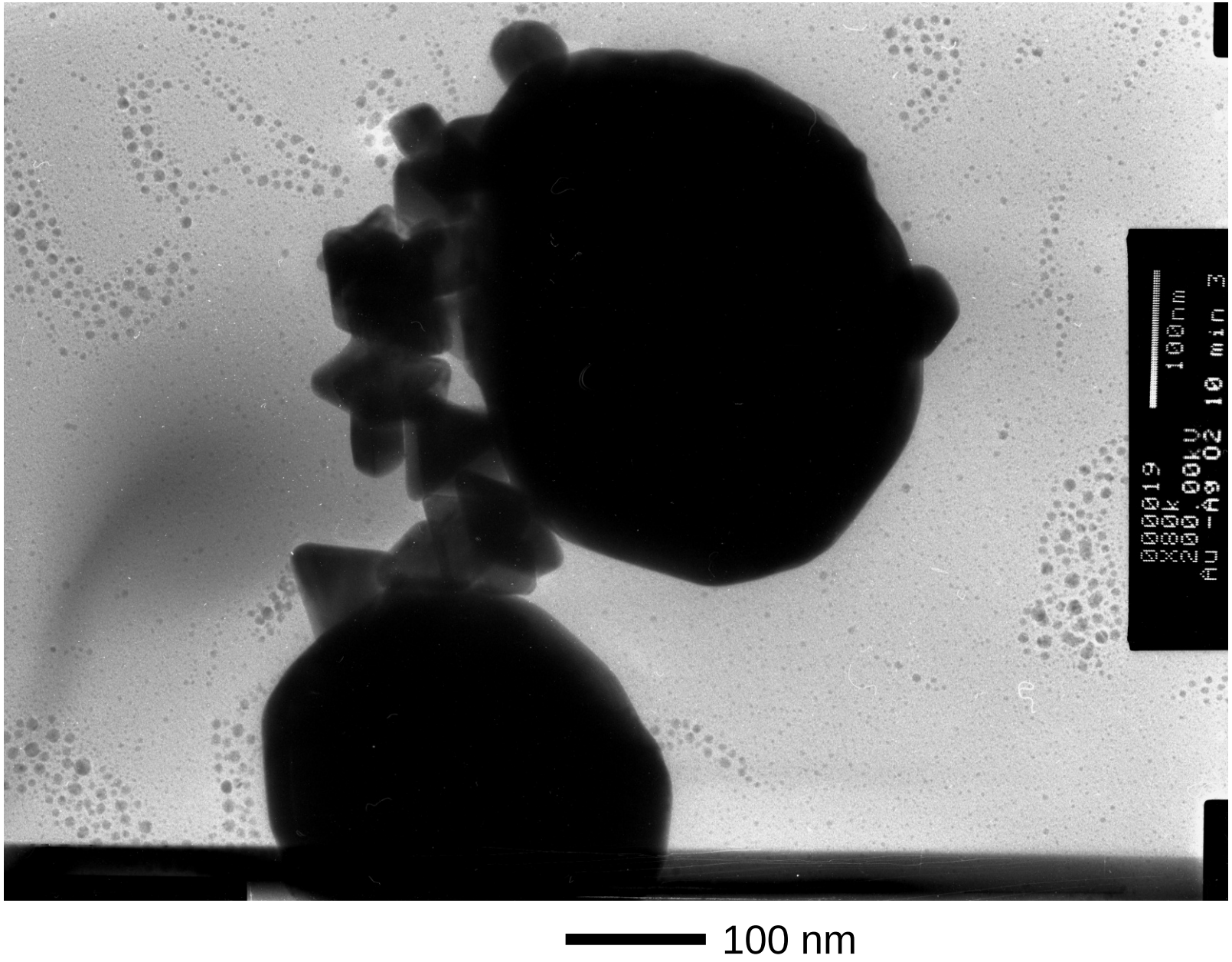

Fig. S6. TEM image of Au–Ag bimetallic products obtained from Au seeds/$AgNO_3$/ PVP/EG solution after heating for 10 min under O_2 gas bubbling.

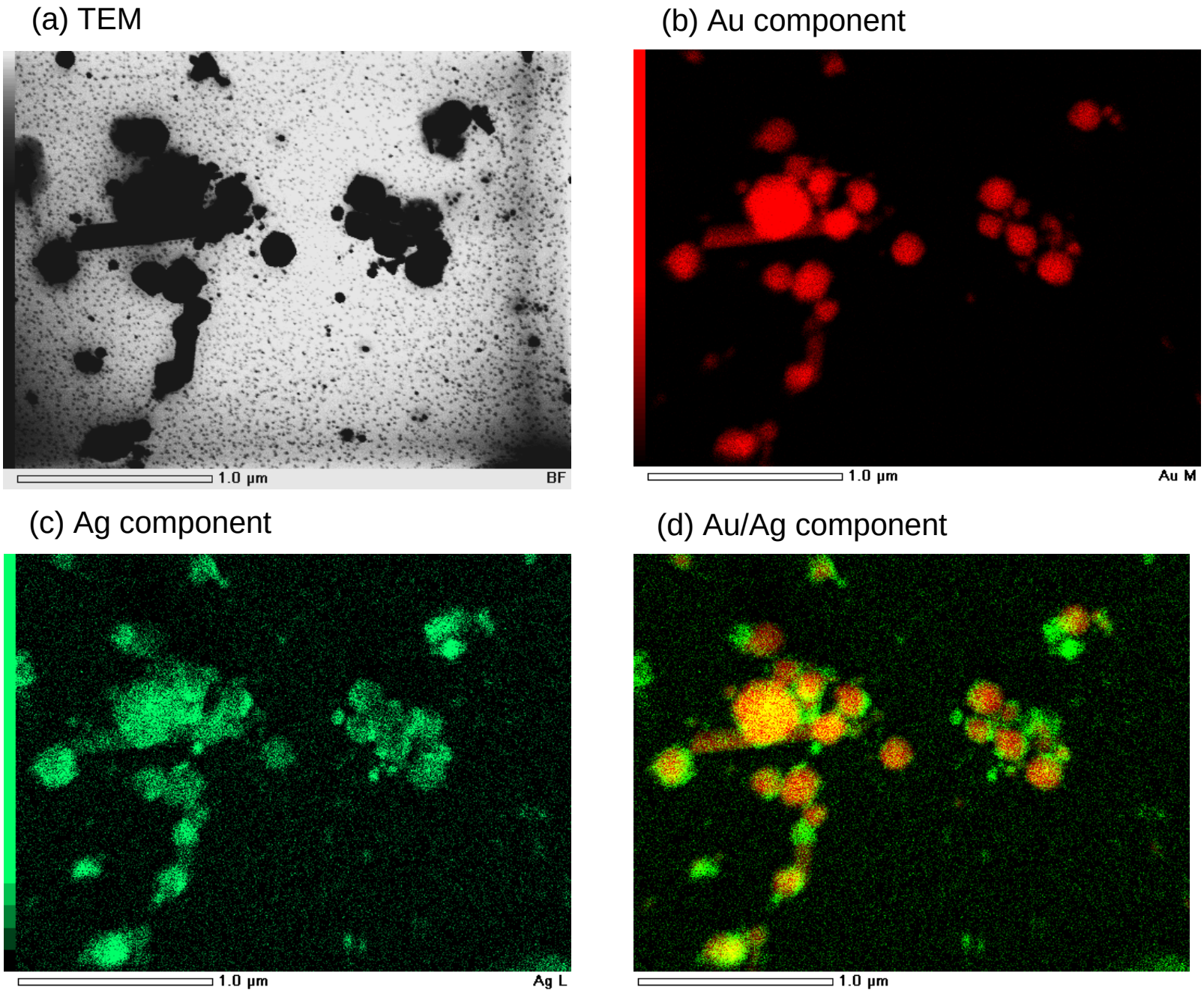

Fig. S7. TEM image of Au–Ag bimetallic particles obtained from Au seeds/$AgNO_3$/ PVP/EG solution after heating for 30 min under O_2 gas bubbling.

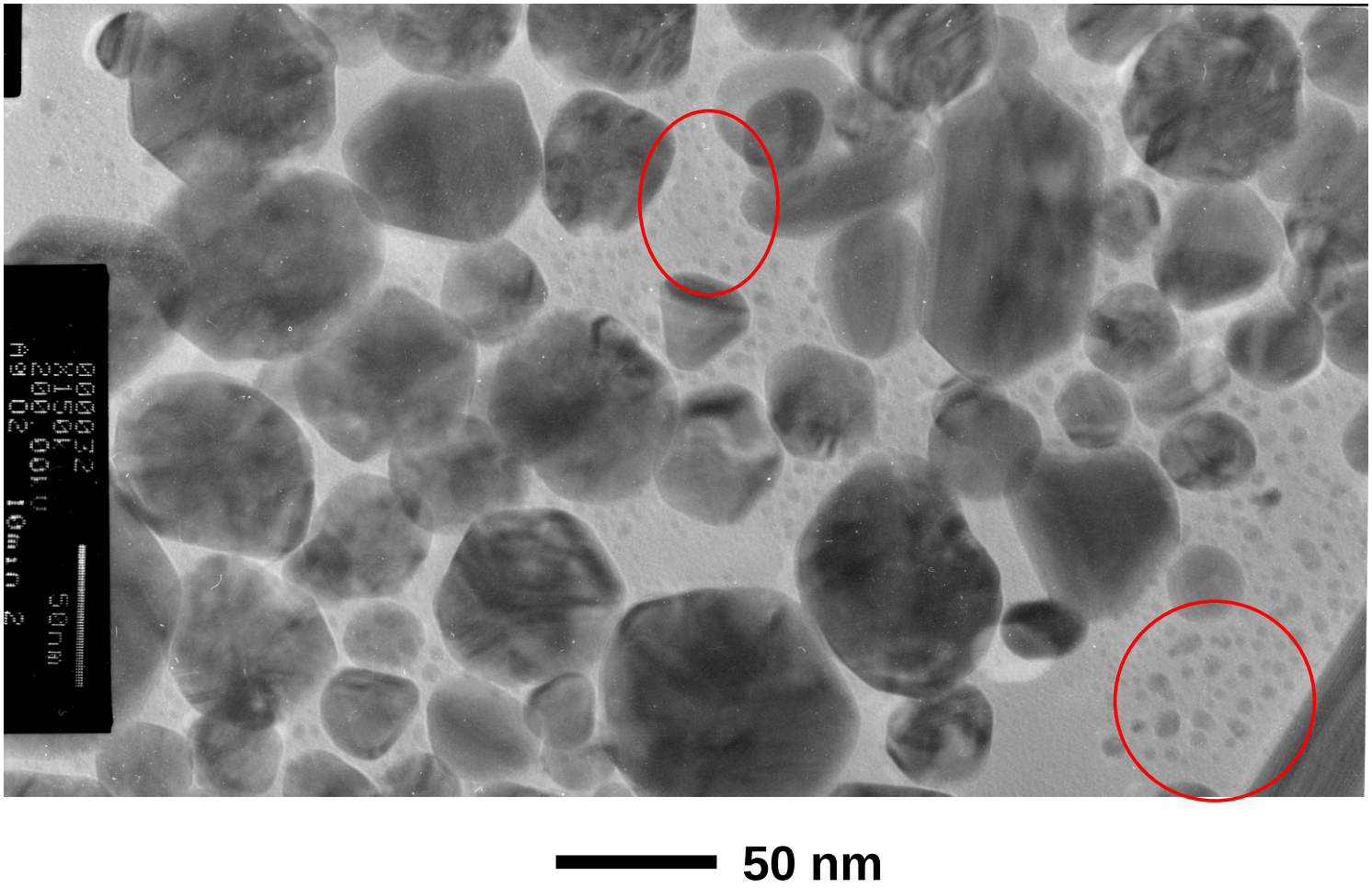

Fig. S8. TEM image of Ag nanoparticles obtained from $AgNO_3$/PVP/EG solution after heating for 10 min under O_2 gas bubbling.

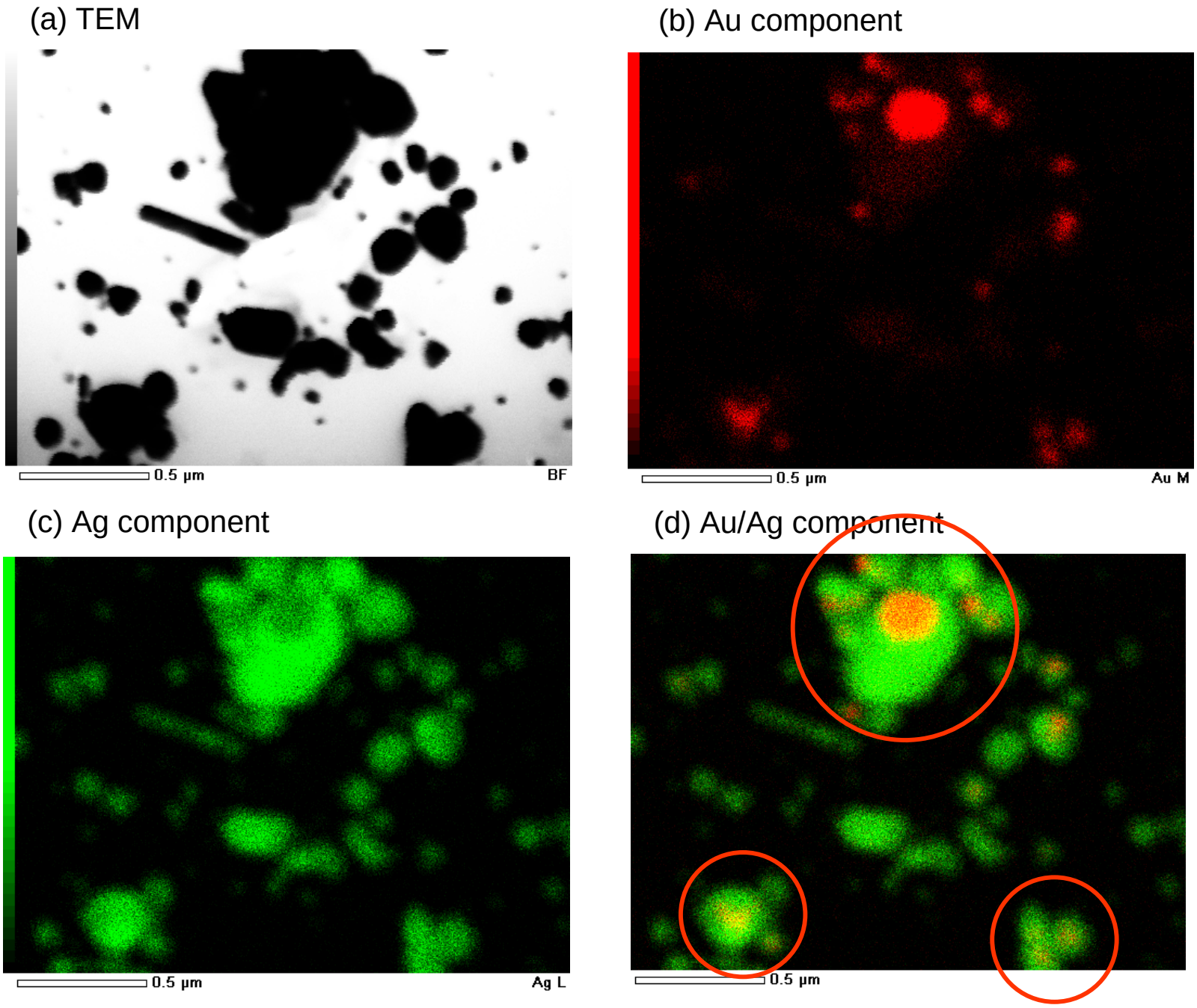

Fig. S9. TEM image of Au–Ag bimetallic particles obtained from Au seeds/ $AgNO_3$/PVP/EG solution after heating for 30 min under Ar gas bubbling.